Mechanisms of spin-dependent dark conductivity in films of a soluble fullerene derivative under bipolar injection

H. Morishita,[1] W. J. Baker,[1] D. P. Waters,[1] R. Baarda,[1] J. M. Lupton,[1,2,*] and C. Boehme[1,†]

[1]*Department of Physics and Astronomy, University of Utah, 115 South 1400 East, Salt Lake City, Utah 84112, USA*

[2]*Institut für Experimentelle und Angewandte Physik, Universität Regensburg, D-93040 Regensburg, Germany*

We report room-temperature pulsed electrically detected magnetic resonance measurements of the dark conductivity of films of the fullerene derivative [6,6]-phenyl-C_{61}-butyric acid methyl ester (PCBM) under bipolar (electron-hole) and unipolar (electron-rich) injection conditions. Directly after material deposition, no detectable spin-dependent processes are observed, yet after storage under ambient conditions for more than a day, two distinct spin-dependent mechanisms are found under bipolar injection, suggesting the involvement of degradation-induced electronic states. Spin-Rabi beat oscillation measurements show that at least one of these processes is due to weakly spin-coupled pairs with $s = 1/2$. The absence of these signals when hole injection is impeded by a barrier suggests that they are due to spin-dependent recombination. The presence of recombination confirms that fullerenes are both electron and hole acceptors, with important consequences for the design, operation, and understanding of plastic solar cells. Electron-hole recombination can occur within homogeneous domains of either the donor or the acceptor of the bulk heterojunction structure, constituting an important dissipative channel in addition to the established interfacial bimolecular recombination loss.

PACS number(s): 71.20.Rv, 76.30.−v, 73.61.−r

I. INTRODUCTION

Fullerene-based compounds are weakly spin-orbit coupled materials, which make electronic processes and therefore macroscopic electrical and optical characteristics strongly dependent on spin-selection rules. As fullerenes have attracted much interest due to their excellent applicability as electron acceptors in organic solar cells [1,2], significant research efforts have focused in the past on how the electron spin degree of freedom can influence the performance of these devices [3,4]. Most studies of spin-selection rules have therefore been centered around transitions of photogenerated charge carriers [5–8] while electronic processes in the dark have received comparatively little attention and only for blend systems [4]. Recently, we reported that pronounced spin-dependent transitions can also exist in the dark current of fullerene films [9]. With the study presented in the following, we aim to provide a more comprehensive picture of this phenomenon. We have investigated spin-dependent transitions under dark conditions in a widely used fullerene derivate, [6,6]-phenyl-C_{61}-butyric acid methyl ester (PCBM). We address the following questions: What is the physical nature of spin-dependent electronic charge carrier transitions that control the macroscopic conductivity in the absence of illumination? Are the spin-dependent transitions observed under electrical injection of excess charge carriers in darkness due to recombination, similar to the well-established spin-dependent recombination [7,8] found for photoinjected carriers in organic semiconductors? Or are these processes due to spin-dependent transport as for instance described by the bipolaron model [10]? Do the observed spin-dependent transitions involve particular paramagnetic defect states (e.g., recombination centers) or are they direct transitions between

charge carrier (polaron) states as known from, e.g., π-conjugated polymers [11–15]?

The motivation for this study is related to recent investigations of spin-dependent processes in organic polymer/fullerene blend materials. Behrends *et al.* [4] reported pronounced spin-dependent signals in the dark current of a poly[2-methoxy-5-(2-ethylhexyloxy)-1,4-phenylenevinylene] (MEH-PPV)/PCBM blend. Under coherent spin excitation, the electric current revealed spin-Rabi beat oscillations that were indicative [16–18] of weakly coupled spin pairs influencing the dark current. While this result is unambiguous, the assignment of these weakly coupled charge carrier pairs to a spin-dependent hole process in the MEH-PPV phase has remained debated [9,19]. This controversy is in part due to the complexity of the blend materials: Spin-dependent signals are known for each of the individual constituent materials of the blend, both involving weakly spin-orbit coupled paramagnetic centers with Landé factors of $g \approx 2$ whose microscopic magnetic resonance signatures are nevertheless broadly distributed due to the omnipresent random hyperfine field in organic semiconductors. Most electron spin resonance line widths of these centers are large enough to cover the range of g factors over which they occur. Given this complexity, it is not clear whether the spin resonant signals that influence the electric current of the blend material involve paramagnetic states and transitions that can occur in either of the blend constituents, or transitions between the blend constituents at intermolecular interfaces (through charge transfer states). The understanding of spin-dependent processes in complex blend materials therefore requires first an understanding of all detectable spin-dependent processes of the individual blend constituents. The study presented here aims to fill this gap for spin-dependent dark currents in PCBM. Although it is well known from electrochemistry and photoconductivity studies that C_{60} films can support radical cations [20–22], the prevailing model of polymer:PCBM blends in photovoltaic devices neglects the possibility of hole injection into the

---

*lupton@physics.utah.edu

†boehme@physics.utah.edu

fullerene. In addition, C_{60} is highly sensitive to oxidation, which can dramatically affect conductivity and magnetic resonance signatures [23,24]. We employ this knowledge here, with a microscopic spectroscopic technique, to demonstrate the nature of bipolar (electron-hole) conduction in fullerene systems.

II. EXPERIMENTAL PROCEDURES

In order to identify spin-dependent electronic transitions which can influence the electrical current, we carried out electrically detected magnetic resonance (EDMR) spectroscopy. The idea is to observe how the spin-degree of freedom controls current by manipulating spins by magnetic resonance and to then observe how this induced spin change modulates the electrical current. EDMR has been applied to various organic materials and device systems in the past [4–9,11–15,25–27]. For this study, we have conducted pulsed (p) EDMR experiments, where the transient of the current change from the steady state is measured after a very short but powerful coherent spin manipulation is performed [28,29]. Pulsed EDMR allows for the observation of coherent spin motion effects such as spin-Rabi nutation during the pulsed excitation. The detection of coherent spin motion then provides insight into the spin Hamiltonian of the observed spin system and thus, very accurately and unambiguously, information about the nature of the investigated spin-dependent mechanism [16–18,30–33].

For the experiments presented in the following, we prepared two types of PCBM thin-film devices: (i) A diode consisting of indium-tin oxide (ITO), poly(3,4-ethylenedioxythiophene) poly(styrenesulfonate) (PEDOT:PSS), PCBM, and aluminum (Al) as illustrated and referred to as "Structure A" in Fig. 1(a). (ii) a diode consisting of ITO, PCBM, and Al as illustrated and referred to as "Structure B" in Fig. 1(b). For the two diodes, qualitative sketches of the band diagrams (in the presence of a bias) are shown in Fig. 1. For the preparation of these structures, commercial ITO coated glass substrates were used on which contact template structures were fabricated whose design allowed for pEDMR experiments in the Bruker X-Band Flexline resonator [11,29] that was used in this study. For Structure A, a thin (<10 nm) film of PEDOT:PSS was spin cast at 2.5 krpm for 40 s before the sample was transferred into a nitrogen purged glove box and annealed at 100 °C for 10 min. An active layer of PCBM was then spin cast at 1.2 krpm for 40 s. Finally, an $\approx$150 nm thick Al layer was deposited by thermal evaporation ($<10^{-5}$ mbar). Structure B was fabricated in the same way except for the PEDOT:PSS deposition step. Devices contained a single pixel of a 2 mm $\times$ 3 mm active area.

For the electrical characterization, the devices were subjected to current-voltage (I–V) measurements directly after fabrication and then repeatedly over a period of six months for Structure A which displayed significant changes of its electrical behavior during the first days after fabrication. Structure B did not display strong changes during the first days and I–V curves were measured up to three weeks after device preparation. The devices were stored under room-temperature atmospheric conditions. The results of the I–V measurements taken on Structure A directly after growth, and one day, five
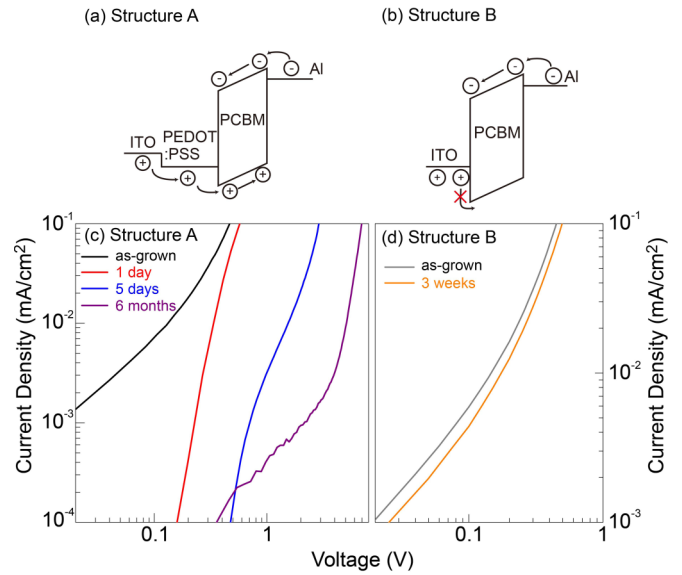

FIG. 1. (Color online) Structure and band diagram of (a) the ITO/PEDOT:PSS/PCBM/Al diode and (b) the ITO/PCBM/Al diode used in this study. (c), (d) Current-voltage characteristics of the device Structure A, B at various times after the device fabrication. While the device with bipolar injection (Structure A) shows significant changes, the device with blocked hole injection (Structure B) shows only marginal changes.

days, and six months later are displayed in Fig. 1(c). The I–V curves of Structure B taken directly after growth and three weeks later are shown in Fig. 1(d).

III. EXPERIMENTAL RESULTS

In order to probe the presence of spin-dependent electronic transitions that control the device current, we conducted one-pulse EDMR experiments for which the transient evolution of the change of the device current from a steady state is measured as a function of an applied magnetic field. When spin-dependent processes influence the current, magnetic resonance induced current changes can be observed at distinct magnetic fields that are governed by the Landé factors of the paramagnetic species involved as well as hyperfine fields in the local environment of these spin states. All measurements discussed in the following were performed at room temperature using a Bruker Elexsys E580 X-band EPR facility equipped with a 5 mm diameter dielectric Flexline resonator.

Figures 2(a) and 2(b) display the small changes $\Delta I(t) = I(t) - I_0$ of the device current $I(t)$ of device Structure A around a steady-state forward current of $I_0 \approx 10 \mu A$ in response to a short (320 ns long) X-band radiation pulse. The two data sets representing two different magnetic field ranges were made six months after fabrication, long after the device had stabilized. The magnetic field region displayed in Fig. 2(a) covers the range of resonant excitation of a Landé factor around $g \approx 2$. The data display significant current changes around magnetic fields of $B_0 \approx 345$ mT. Superimposed on Fig. 2(a) are plots of $\Delta I(t)$ for $t = 20 \mu s$, $t = 50 \mu s$, and $t = 70 \mu s$. They reveal that the magnetic field dependencies
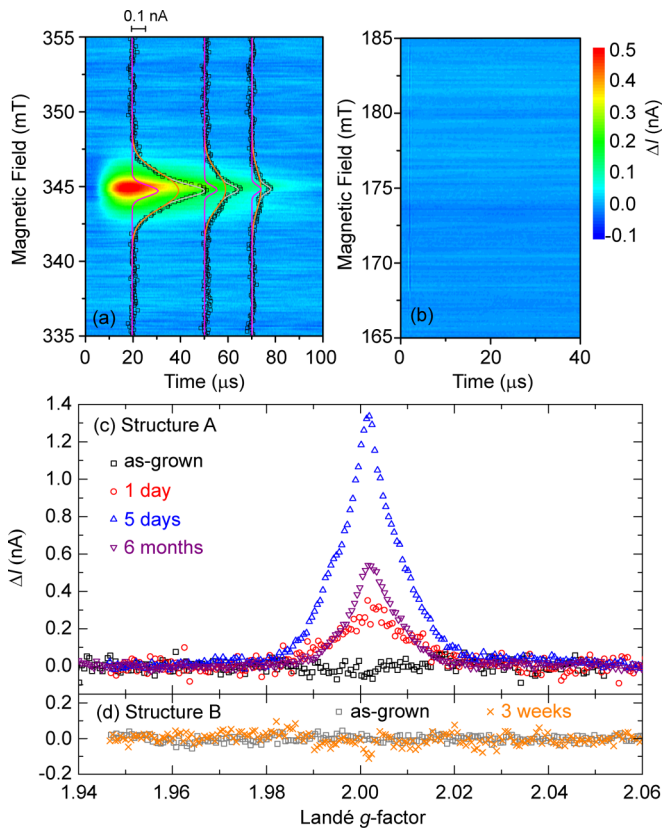
FIG. 2. (Color online) (a), (b) Color plots of the current change ΔI from an applied steady-state current after an X-band (≈ 9.7 GHz) microwave pulse of 320 ns length and ≈ 10 W power was applied at a time $t = 0$, as a function of time t after the pulse and applied magnetic field B_0. The data was recorded when the device was six months old. (a) At $B_0 \approx 345$ mT, a transient response of the device current is observable indicating the existence of spin-dependent processes. (b) No significant current change was observed at around $B_0 \approx 175$ mT, the anticipated magnetic field range for half-field resonances induced by the triplet excited state. (c), (d) Maximal current changes observed at $t = 20 \mu s$ after the excitation as a function of Landé factor of resonant excitation for the two sample structures and sample ages corresponding to the data of Fig. 1. In general, newly prepared and electron-only devices never showed spin-dependent signals.

of these current changes can consistently be well fit by two mutually different Gaussian distributions. For each time t, the two Gaussian functions turned out to show the same widths of 0.72(9) mT and 2.85(11) mT with nearly identical centers around $g = 2.0031(2)$ and $2.0030(2)$, respectively. However, the absolute magnitudes of these two Gaussians did show a strong t dependence, along with the ratios of both the magnitudes as well as the integrated areas of the two peaks. EDMR spectra arising from spin-dependent transitions within charge carrier pairs always consist of two resonance peaks with equal peak area and constant ratios between the peak intensities, independent of the time t after resonant excitation. The results for PCBM shown in Fig. 2, which do not display equal peak areas at all, therefore indicate that either several different spin-dependent pair processes must be involved in the signal shown by Fig. 2(a); or alternatively a process that does not involve weakly interacting spin pairs,

such as interaction with a spin center like an ion, is present. Figure 2(b) displays pEDMR data recorded on the same sample and under the same conditions as for Fig. 2(a) but within a magnetic field range around $g \approx 4$, which is known to include magnetic resonances of strongly dipolar coupled triplet states [14,27]. The data does not reveal any detectable spin-dependent signal above the noise level of $\delta I \approx 40$ pA, corresponding to a relative sensitivity of $\delta I/I_0 \approx 4 \times 10^{-6}$. From this observation one can therefore directly conclude that spin-dependent transitions such as the triplet-polaron process, which is known to influence conductivity in π-conjugated polymers at low temperatures [14,27], do not affect the dark conductivity of PCBM at room temperature.

Figures 2(c) and 2(d) display the results of the repetition of the experiments in Fig. 2(a) for younger sample ages, those for which I–V curves are shown in Fig. 1. These measurements demonstrate that for both sample structures, no significant spin-dependent signals can be observed directly after sample fabrication. For the electron rich device (Structure B), this never changes for any of the investigated sample ages. In contrast, the electron-hole injection device given by Structure A reveals spin-dependent signals after one day of aging. The signals then increase over the following days until a maximum is reached after about five days. Thereafter, the EDMR signals decrease over a period of several months. These observations indicate that after fabrication, microscopic changes occur within the device, which are responsible for the observed spin-dependent processes. It should be noted that while the magnitudes of the observed spin-dependent signals change as a function of device age, the line shapes of the two resonances remain unchanged. The two widths remain constant within the error margins. The double-Gaussian resonances shown in the data of Fig. 2 are well known from spin-dependent processes of other organic semiconductors where the two peaks are assigned to electrons and holes, respectively (e.g., electron- and hole-polaron states in MEH-PPV [12]). From the absence of any detectable spin-dependent signal in the device with electrons as majority charge carriers (Structure B), we conclude that for spin-dependent signals to appear in neat PCBM, both electrons and holes must be present. Note that we can exclude spin-dependent currents caused by PEDOT:PSS as the origin of the observed signals in Structure A devices as we have previously shown that PEDOT:PSS does not exhibit any spin-dependent transitions at room temperature [9]. Because of this, the two resonances observed in Structure A can be attributed to electrons and holes. The spin-dependent process in which these charge carriers are involved is therefore recombination.

In order to learn more about the nature of the spin-dependent processes found in Structure A, we conducted electrically detected spin-Rabi oscillation measurements. For this, the magnitude of spin-resonantly perturbed sample currents is measured as a function of the applied pulse length τ. The coherent precession of the spin states involved in spin-dependent transitions (the spin-Rabi oscillation) is then revealed [16] as an oscillation of the pEDMR-signal as a function of τ. The oscillation frequencies give insights into the nature of the involved spin-dependent process. This spin-Rabi oscillation spectroscopy has been developed both experimentally as well as theoretically in the past decade [17,18,30–33] and it has
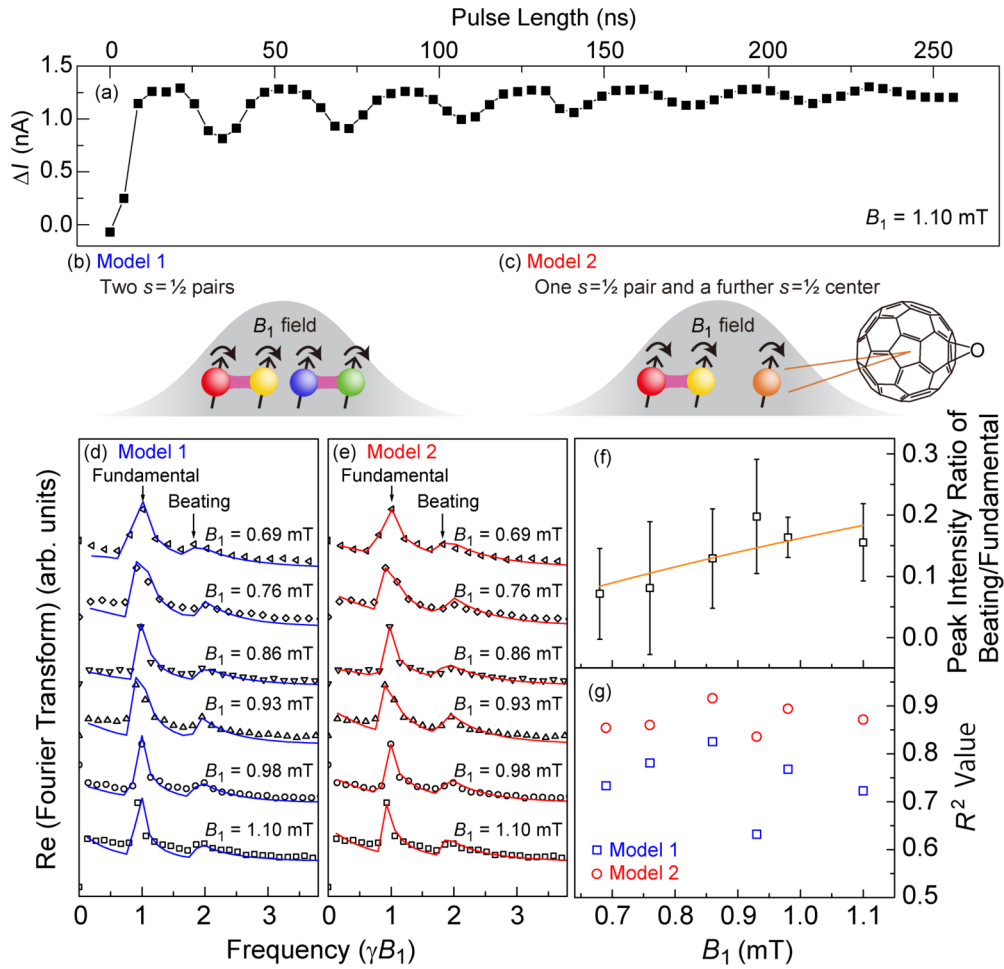
FIG. 3. (Color online) (a) The current change ΔI of a Structure A device measured at a time $t = 20\mu$s after application of resonant microwave pulses with $B_1 = 1.1$ mT as a function of the pulse length τ shows coherent control by spin-Rabi oscillation. (b), (c) Sketches of the two hypotheses (Models 1 and 2, respectively), which are tested in order to explain the observed spin-dependent process. Model 1 describes the presence of two independent pair processes of weakly interacting charge carrier pairs while Model 2 assumes one pair process and one process for which only a weakly interacting paramagnetic center (such as an oxidative defect) with spin $s = 1/2$ is observed. (d), (e) Plots of the real components of the Fourier transforms of the data in (a) and other spin-Rabi oscillation measurements recorded for different driving field strengths B_1. The blue and red plots represent fits of the data based on the different models. (f) Plot of the ratio of the peak intensities of the $2\gamma B_1$ harmonic in the Fourier transform to the fundamental γB_1 as a function of the applied driving field B_1. (g) Plot of the coefficient of determination R^2 for both models 1 and 2 as a function of the applied driving field B_1.

been shown that it is capable of identifying the spin manifold that is involved in an observed process (i.e., the underlying spin Hamiltonian) as well as the nature of spin coupling to the environment [4,12,29,34].

Figure 3 illustrates the results of the Rabi-oscillation measurements conducted on the EDMR signal measured on a Structure A device. The displayed data was measured at an arbitrary time of one month after the device preparation. We also conducted the same experiments 10 days after device preparation. These measurements revealed that while the EDMR signal magnitude changes slightly in magnitude as a function of the sample age as indicated in Fig. 2, there is no change of the relative magnitudes (= normalized magnitudes) of the Rabi oscillation components. The conclusions drawn from these measurements in the following therefore apply to different sample ages and it appears that they apply to all sample ages where spin-dependent signals are visible. Figure 3(a) displays the change ΔI of the sample current

measured after a time $t = 20\mu$s as a function of pulse length τ. For the applied strength B_1 of the resonant driving field, a pronounced oscillatory behavior is revealed, an imprint of the coherent spin motion of the paramagnetic centers involved in spin-dependent transitions controlling the sample current. We repeated this experiment for various strengths of B_1, which caused the observed spin-Rabi oscillations to occur with different frequencies. In order to inspect the harmonic components of these different experiments, the real components of the Fourier transformations of these pulse-length-dependent measurements are displayed in Figs. 3(d) and 3(e).

IV. ANALYSIS OF EXPERIMENTAL RESULTS

The Fourier transformations shown in Fig. 3 reveal two pronounced harmonic components with frequencies γB_1 corresponding to the fundamental spin $s = 1/2$ Rabi frequency

(the strong peak) and $2\gamma B_1$ (the weaker peak) that is known to relate to the relative propagation of spin $s = 1/2$ pairs, referred to in the literature as spin-Rabi beat oscillation [12] or spin locking [4]. Here, γ is the gyromagnetic ratio. The occurrence of a beat frequency of $2\gamma B_1$ requires very weak spin-dipolar interaction between the pair partners [33] since both spins must precess independently of each other. However, it can occur in the presence or in absence of spin exchange [30,32]. Given strong spin exchange (the exchange integral J exceeds the spin resonance frequency difference $\Delta\omega$ within the pair partners), the magnitude of the beat oscillation signal is expected to be independent of the driving field strengths B_1 and significantly stronger than the fundamental oscillation [30]. With weak spin exchange ($J \ll \Delta\omega$), the beat oscillation is absent when $B_1 \ll \Delta\omega$ and very pronounced when $B_1 \gg \Delta\omega$. Figure 3(f) displays the ratio of the magnitudes (the peak maxima) of the spin-Rabi beat oscillation component to the fundamental oscillation component as a function of B_1. Based on the consistently low ratio for any of the applied B_1 fields, we can exclude the possibility that strongly exchange coupled pair partners are involved in the observed signal as we would anticipate the peak ratios to far exceed unity for all applied B_1 fields [30]. We therefore apply a fit function to the dependence of fundamental to harmonic peak ratio on B_1 for weakly spin-exchange and dipolar coupled pairs [orange line in Fig. 3(f)]. This fit derives from the resonance peak widths obtained from the data in Fig. 2(a) following the procedure described by Lee *et al*. [35]. There is reasonable agreement between the fit and the experimental data. However, the consistently low values of the harmonic to fundamental amplitude ratio even for B_1 fields that exceed the width of the narrow resonance line in Fig. 2(a) suggest that a pair mechanism involving narrow and broad resonance peaks is not the only spin-dependent process responsible for the detected signals. Following the agreement of the fit function with the experimental data in Fig. 3(f), we also attempted to fit the Fourier spectra in Figs. 3(d) and 3(e) with the analytically known frequency spectral function [18] for a single-pair process with pair partner resonances arising from the two Gaussian resonances revealed in Fig. 2(a). These fits show consistently poor agreement (not shown here, the coefficients of determination for all fit attempts were below 0.5) suggesting again that a single-pair process is not alone responsible for the observed spin-dependent current.

From the data shown in Figs. 2 and 3, we have excluded that we observe (i) a single spin-dependent electronic process, (ii) spin-dependent transport of electrons, (iii) processes involving triplet excitons, and (iv) recombination through strongly spin-exchange coupled pairs. We therefore conclude that more than one spin-dependent process must be responsible for the observed data. This conclusion is also supported by the observation revealed in Fig. 2 where the two resonance peaks (Gaussian fit functions) display different dynamic behavior and significantly different integrated peak intensities. Given the presence of the weak beat oscillation component in the Rabi-oscillation measurement that increases slightly with B_1, we arrive at the hypothesis that there must be at least two spin-dependent processes present. At least one of these must be due to weakly spin-spin coupled $s = 1/2$ pairs to account for the beating behavior. The other process could be due to a different kind of pair of $s = 1/2$ states (i.e., pairs with different

resonance peaks and, therefore, a different beat behavior), but it could also be a spin-dependent process, which involves paramagnetic states with $s = 1/2$ but not pairs (i.e. such a process would not exhibit beating). These two remaining hypotheses are illustrated in Figs. 3(b) and 3(c) as Model 1 and Model 2, respectively. We have scrutinized these two cases by fits of the experimentally obtained spin-Rabi oscillation data. Figures 3(d) and 3(e) show identical experimental data sets but two different fits, which correspond to the two models 1 and 2. The fit function of Model 1 consists of a superposition of two independent pair processes of weakly interacting pairs. The two pair systems consist of $\Delta\omega$ distributions corresponding to (i) pairs due to the narrow weak peak and the broad strong resonance peak seen in Fig. 2(a); and (ii) pairs where both pair partners are subjected to the resonance distribution of the broad peak with 3.26(37) mT widths (the peak width controls the B_1 threshold for the occurrence of spin beating). This peak is significantly broader than the magnitude of the strongest experimentally available B_1 field of 1.1 mT. Hence, a detectable beat oscillation would not be expected in our experiment from the large (in area) and broad resonance peak, even if it was due to charge carrier pairs. In contrast, for Model 2, we have assumed that the spin-dependent signal seen is solely due to an $s = 1/2$ system, which only causes an $s = 1/2$ nutation component. Physical implementations of spin-dependent processes exhibiting this behavior could be expected for instance from spin-dependent hopping processes [14] or again, weakly coupled pairs where one of the two pair partners has a resonance frequency that is far removed from the broad resonance peak. Such a situation may conceivably occur when the g factor of C_{60} is shifted due to oxidation [23], which effectively corresponds to doping. The fit results for the two models are shown in Figs. 3(d) and 3(e) and the coefficients of determination R^2 for these fits of both models to all data sets are plotted in Fig. 3(g). Model 2 clearly displays consistently better agreement with all data sets.

V. DISCUSSION AND CONCLUSIONS

We find that the room-temperature dark current of neat PCBM films is influenced by at least two different spin-dependent charge carrier recombination processes, which involve states with $s = 1/2$ as long as bipolar charge carrier injection (of electrons and holes) occurs and the device is stored for at least a day after fabrication, presumably promoting oxidation. For electron-only PCBM devices, without a sufficiently low-work function anode, we did not see detectable spin-dependent currents even three weeks after fabrication. Triplet states are not involved in the detected spin-dependent processes of bipolar devices since no half-field resonance is seen. The electrical detection of spin-Rabi oscillations shows that one of the two processes is due to pairs of the two detected $s = 1/2$ species. Since the spin-dependent signals emerge only over the course of days after device fabrication, we surmise that the observed spin species are electrons and holes trapped at point defects (such as those formed by oxygen complexation [23]), which act as recombination centers and which are gradually generated as a device is stored in an atmospheric environment. The nature of the second spin-dependent process is not as clear: Our data do

not support the hypothesis that spin-dependent processes are related to $s = 1/2$ pairs whose pair partners are both associated with the broad resonance peak. Instead, we believe that this second process is either due to a single $s = 1/2$ species different from the broad peak and not directly resolved in the resonance spectrum in Fig. 2 or it is due to a pair in which one pair partner is related to the broad resonance peak and the other pair partner is unknown (e.g., of ionic origin) but not related to either the broad or the narrow peak. Note that this insight implies that spin-dependent transport through pairs of qualitatively identical partners is unlikely. While our data obtained from the bipolar devices prove that holes can be injected into PCBM, and can indeed control the majority current of electrons, we expect that spin-dependent hole transport is unlikely to be significant, owing to the low hole mobility in PCBM [24]. While PCBM is usually considered a pure electron acceptor and electron transporter, our experiments confirm independently (with entirely distinct spectroscopies) previous studies [22–24] that have shown that C_{60} is very able to accept holes in spite of its low hole mobility and low-lying highest-occupied molecular orbital, and can thus support electron-hole recombination. This knowledge, along with the exceptional sensitivity to material aging, is crucial for developing a microscopic picture of recombination losses in solar cells in general, and spin-dependent transport in blend systems in particular [4]. Notably, electron-hole recombination constitutes a possible loss channel within the C_{60} domains of bulk heterojunctions, occurring on top of donor-acceptor interfacial bimolecular recombination. Finally, we conclude that the measurements of spin beating by Behrends *et al.* [4] most likely comprise a superposition of PCMB and MEH-PPV spin resonance features, rather than constituting a manifestation of bipolaronic (hole-hole pair) resonance within the MEH-PPV. Ultimately, this finding is not surprising since it is hard to conceive how two holes should be able to attract each other sufficiently strongly, within a continuous polymer matrix, as proposed by Behrends, so as to form a distinct resonance species. In contrast, an intrachromophoric bipolaron would be strongly exchange coupled and would therefore not exhibit a transition from non-beating to beating.

[1] N. S. Sariciftci, L. Smilowitz, A. J. Heeger, and F. Wudl, Science **258**, 1474 (1992).

[2] C. J. Brabec, N. S. Sariciftci, and J. C. Hummelen, Adv. Funct. Mater. **11**, 15 (2001).

[3] X. Wei, Z. V. Vardeny, N. S. Sariciftci, and A. J. Heeger, Phys. Rev. B **53**, 2187 (1996).

[4] J. Behrends, A. Schnegg, K. Lips, E. A. Thomsen, A. K. Pandey, I. D. W. Samuel, and D. J. Keeble, Phys. Rev. Lett. **105**, 176601 (2010).

[5] I. Hiromitsu, Y. Kaimori, M. Kitano, and T. Ito, Phys. Rev. B **59**, 2151 (1999).

[6] I. Hiromitsu, Y. Kaimori, M. Kitano, R. Shinto, and T. Ito, Synth. Met. **102**, 1439 (1999).

[7] T. Eickelkamp, S. Roth, and M. Mehring, Mol. Phys. **95**, 967 (1998).

[8] W. Harneit, C. Boehme, S. Schaefer, K. Huebener, K. Fostiropoulos, and K. Lips, Phys. Rev. Lett. **98**, 216601 (2007).

[9] C. Boehme and J. M. Lupton, Nature Nanotechnol. **8**, 612 (2013).

[10] P. A. Bobbert, T. D. Nguyen, F. W. A. van Oost, B. Koopmans, and M. Wohlgenannt, Phys. Rev. Lett. **99**, 216801 (2007).

[11] D. R. McCamey, H. A. Seipel, S.-Y. Paik, M. J. Walter, N. J. Borys, J. M. Lupton, and C. Boehme, Nature Mater. **7**, 723 (2008).

[12] D. R. McCamey, K. J. van Schooten, W. J. Baker, S.-Y. Lee, S.-Y. Paik, J. M. Lupton, and C. Boehme, Phys. Rev. Lett. **104**, 017601 (2010).

[13] D. R. McCamey, S.-Y. Lee, S.-Y. Paik, J. M. Lupton, and C. Boehme, Phys. Rev. B **82**, 125206 (2010).

[14] W. J. Baker, D. R. McCamey, K. J. van Schooten, J. M. Lupton, and C. Boehme, Phys. Rev. B **84**, 165205 (2011).

[15] W. J. Baker, T. L. Keevers, J. M. Lupton, D. R. McCamey, and C. Boehme, Phys. Rev. Lett. **108**, 267601 (2012).

[16] C. Boehme and K. Lips, Phys. Rev. B **68**, 245105 (2003).

[17] V. Rajevac, C. Boehme, C. Michel, A. Gliesche, K. Lips, S. D. Baranovskii, and P. Thomas, Phys. Rev. B **74**, 245206 (2006).

[18] R. Glenn, W. J. Baker, C. Boehme, and M. E. Raikh, Phys. Rev. B **87**, 155208 (2013).

[19] J. Behrends, I. D. W. Samuel, A. Schnegg, and D. J. Keeble, Nature Nanotechnol. **8**, 884 (2013).

[20] J. Kalinowski, G. Giro, N. Camaioni, V. Fattori, and P. Di Marco, Synthetic Met. **77**, 181 (1996).

[21] R. Könenkamp, J. Erxmeyer, and A. Weidinger, Appl. Phys. Lett. **65**, 758 (1994).

[22] C. Jehoulet, A. J. Bard, and F. Wudl, J. Am. Chem. Soc. **113**, 5456 (1991).

[23] P. Paul, K.-C. Kim, D. Sun, P. D. W. Boyd, and C. A. Reed, J. Am. Chem. Soc. **124**, 4394 (2002).

[24] R. Könenkamp, G. Priebe, and B. Pietzak, Phys. Rev. B **60**, 11804 (1999).

[25] V. Dyakonov, N. Gauss, G. Rösler, S. Karg, W. Rieß, and M. Schwoerer, Chem. Phys. **189**, 687 (1994).

[26] G. B. Silva, L. F. Santos, R. M. Faria, and C. F. O. Graeff, Physica B **308–310**, 1078 (2001).

[27] J. Shinar, Laser Photonics Rev. **6**, 767 (2012).

[28] J. M. Lupton, D. R. McCamey, and C. Boehme, Chem. Phys. Chem. **11**, 3040 (2010).

[29] C. Boehme, D. R. McCamey, K. J. van Schooten, W. J. Baker, S.-Y. Lee, S.-Y. Paik, and J. M. Lupton, Phys. Status Solidi (b) **246**, 2750 (2009).

[30] A. Gliesche, C. Michel, V. Rajevac, K. Lips, S. D. Baranovskii, F. Gebhard, and C. Boehme, Phys. Rev. B **77**, 245206 (2008).

[31] C. Michel, A. Gliesche, S. D. Baranovskii, K. Lips, F. Gebhard, and C. Boehme, Phys. Rev. B **79**, 052201 (2009).

[32] R. Glenn, M. E. Limes, B. Saam, C. Boehme, and M. E. Raikh, Phys. Rev. B **87**, 165205 (2013).

[33] M. E. Limes, J. Wang, W. J. Baker, S.-Y. Lee, B. Saam, and C. Boehme, Phys. Rev. B **87**, 165204 (2013).

[34] S. Schaefer, S. Saremi, K. Fostiropoulos, J. Behrends, K. Lips, and W. Harneit, Phys. Status Solidi (b) **245**, 2120 (2008).

[35] S.-Y. Lee, S.-Y. Paik, D. R. McCamey, J. Yu, P. L. Burn, J. M. Lupton, and C. Boehme, J. Am. Chem. Soc. **133**, 2019 (2011).